BIBECHANA
Vol. 22, No. 3, December 2025, 280–290

ISSN 2091-0762 (Print), 2382-5340 (Online)
Journal homepage: http://nepjol.info/index.php/BIBECHANA
Publisher:Dept. of Phys., Mahendra Morang A. M. Campus (Tribhuvan University)Biratnagar

Thermodynamic and surface properties of Al-Cu-Fe-Si-Ti liquid alloy

N. Dahal[1,2,3], U. Mehta[2], R. K. Gohivar[2], R. P. Koirala[2], S. K. Yadav[2]*

[1]*Central Department of Physics,Tribhuvan University, Kirtipur*
[2]*Department of Physics, Mahendra Morang Adarsh Multiple Campus, Tribhuvan University Biratnagar, Nepal.*
[3]*Department of Physics,Sukuna Multiple Campus,Tribhuvan University, Sundarharaincha*
*Corresponding author. Email: sashit.yadav@mmamc.tu.edu.np

Abstract

The thermodynamic and surface properties of the Al-Cu-Fe-Si-Ti liquid alloy were systematically investigated using theoretical models. These properties were investigated at different cross-sections from Fe and Ti corners. For the comparative study, the excess Gibbs free energy of mixing for the liquid alloy was determined using the Muggianu, Kohler, and Chou models, based on the thermodynamic database of constituent binary subsystems available in the literature. The activity of the system was calculated using Chou model. The activities of Al, Fe, Si, and Ti showed negative deviations from Raoult's law, confirming strong complex-forming tendencies, whereas Cu exhibited positive deviations, highlighting its weaker interaction and tendency toward segregation. These deviations diminished with increasing temperature, indicating that elevated thermal energy reduces ordering interactions and promotes random mixing. The surface tension of the alloy was calculated using Butler equation with the aid of thermodynamic database. Present investigations revealed that compositions enriched with elements of intrinsically higher surface tension exhibited larger overall surface tension values. Surface segregation studies demonstrated that Al possesses the strongest surface affinity, followed by Si, while Ti is the least surface-active element. These findings provide crucial insights into the thermodynamic stability and interfacial behavior of multicomponent Al–Cu–Fe–Si–Ti liquid alloys, which are essential for optimizing their processing and applications.

Keywords
Al-Cu-Fe-Si alloy, Chou model, thermodynamic modeling, R-K polynomial, surface tension.

Article information
Manuscript received: August 19, 2025; Revised: September 9, 2025; Accepted: September 12, 2025
DOI https://doi.org/10.3126/bibechana.v22i3.83332

1 Introduction

The development of alloys has been driven by the need to engineer materials with tailored properties for scientific and technological applications. Among these, Al-based multicomponent alloys are widely used in aerospace and automotive industries due to their lightweight, high strength, wear resistance, and cost-effectiveness [1]. Their recyclability properties further make them superior to polymer-based materials. The addition of Fe to Al enhances mechanical strength [2], while Al-Cu alloys can form quasicrystalline structures, exhibiting low thermal conductivity and high corrosion resistance [3]. Incorporating Si into Al-Cu-Fe alloys promotes quasicrystalline phase formation, improving fluidity, reducing porosity, and enhancing strength [4–6] . Similarly, Ti-based alloys are favored in aeronautics and aerospace for their high strength-to-weight ratio, low density, excellent corrosion resistance and high melting temperature. However, their poor oxidation resistance at high temperatures can be mitigated by surface modification, where Ti concentration is reduced by alloying with oxidation-resistant elements that preferentially segregate to the surface [7]. Experimental investigation of alloys in molten states faces significant challenges, including high reactivity of elements at elevated temperatures, time-consuming procedures, high costs, and the need for advanced instrumentation [8]. The theoretical modeling complements the experimental study by exploring a vast range of compositions and temperature-dependent structures, saving time and resources. In this regard, different theoretical models such as Collinet [9], Hillert [9, 10], Kohler [9, 11, 12], Muggianu [9, 12, 13], Toop [11, 12, 14] and Chou's (also known as General Solution Model, GSM) [12, 15, 16] models are collectively recognized as geometric models, have been developed to explore mixing properties of ternary and higher order liquid alloys. Notably, the Chou model and symmetric geometric models like Muggianu and Kohler are often considered more appropriate than asymmetric geometric models for analyzing highly intricate multi-component alloys [9]. These computational approaches have been widely employed to assess the thermo-physical properties of ternary liquid alloys [11–14, 17, 18] and quaternary systems [8, 19–21]. Notably, Arslan and Dogan [9] applied these models to predict the thermodynamic behavior of the Fe-Cr-Ni-Mg-O quinary system, while Dogan et al. [13] investigated the Ni-Cr-Co-Al-Mo system. Extending this further, Dogan and Arslan [22] analyzed the Ni-Cr-Co-Al-Mo-Ti-Cu system, leveraging thermodynamic databases of constituent binary subsystems to enhance predictive accuracy. Moreover, a comprehensive investigation of the Al-Cu-Fe-Si-Ti liquid alloy remains unexplored, with no theoretical or experimental data reported to date.

Therefore, this study is designed to explore the thermodynamic and surface properties of Al-Cu-Fe-Si-Ti liquid alloy using theoretical modeling equations. The common fundamental concept of these models is that the behavior of alloys is the cumulative effects of their binary subsystems with a specific weightage assigned to each.

2 Formalism

2.1 Thermodynamics properties

Excess Gibbs free energy of mixing ΔG_M^{xs} is a thermodynamic function that has a strong influence on the mixing behavior of alloys. For binary liquid alloys, the respective parameter ΔG_{ij}^{xs} is expressed in the form of Redlich-Kister (R-K) polynomial as [10–12, 23]

$$\Delta G_{ij}^{xs} = X_i X_j \sum A_{ij}^{\nu} (X_i - X_j)^{\nu} \tag{1}$$

where X_i and X_i are the concentrations of the components in the binary alloys. A_{ij}^{ν} are the coefficients of the R-K polynomials.

The expression for ΔG_M^{xs} of multi-component liquid alloy is obtained by adding ΔG_{ij}^{xs} with suitable probability weight assigned to each [11, 14, 20, 21, 24]

$$\Delta G_M^{xs} = \Sigma_{ij,i\neq j}^{m} W_{ij} \Delta G_{ij}^{xs} \tag{2}$$

where, $i, j = 1, 2, 3, ...m$ depending upon the components of the alloy. For quinary alloy, m=5 and hence ΔG_M^{xs} can be expressed as

$$\begin{aligned} \Delta G_M^{xs} = {} & W_{12}\Delta G_{12}^{xs} + W_{13}\Delta G_{13}^{xs} + W_{14}\Delta G_{14}^{xs} \\ & + W_{15}\Delta G_{15}^{xs} + W_{23}\Delta G_{23}^{xs} + W_{24}\Delta G_{24}^{xs} \\ & + W_{25}\Delta G_{25}^{xs} + W_{34}\Delta G_{34}^{xs} + W_{35}\Delta G_{35}^{xs} \\ & + W_{45}\Delta G_{45}^{xs} \end{aligned} \tag{3}$$

The term W_{ij} is the probability weight assigned to binary pairs of the multi-component alloy, expressed as

$$W_{ij} = \frac{x_i x_j}{X_{i(ij)} X_{j(ij)}} \tag{4}$$

where x_i and x_j are the concentrations of the components in the quinary system and X_i and X_j are the concentrations of the components in the constituent binary subsystem. The selection of later two terms depends upon the preferred theoretical model. For example,
Muggianu model [9, 13]

$$\begin{aligned} X_{i(ij)} &= \left(\frac{1 + x_i - x_j}{2}\right), \\ X_{j(ij)} &= \left(\frac{1 + x_j - x_i}{2}\right) \end{aligned} \tag{5}$$

Kohler model [9, 13]

$$X_{i(ij)} = \frac{x_i}{x_i + x_j}, X_{j(ij)} = \frac{x_j}{x_i + x_j} \quad (6)$$

Chou model [9, 13]

$$X_{i(ij)} = x_i + \Sigma^m_{k=1,k\neq i,j} x^k \xi^k_{i(ij)} \quad (7)$$

Herein, $\xi^k_{i(ij)}$ are the similarity indices of component k to component i in ij subsystem, expressed as [14, 17, 21]

$$\xi^k_{i(ij)} = \frac{\eta(ij, ik)}{\eta(ij, ik) + \eta(ji, jk)} \quad (8)$$

The term $\eta_{(ij,ik)}$ in Equation (8) is the square of deviation, expressed in the form

$$\eta_{(ij,ik)} = \int_0^1 (\Delta G^{xs}_{ij} - \Delta G^{xs}_{ik})^2 dX_i \quad (9)$$

The activity coefficient γ_i of i^{th} component in the multi-component liquid alloy is related to partial excess Gibbs free energy (ΔG^{xs}_i) as [12, 25]

$$RT \ln \gamma_i = \Delta G^{xs}_i \quad (10a)$$

Once γ_i is calculated, the activity (a_i) of the respective component can be calculated using the relation

$$a_i = x_i \gamma_i \quad (10b)$$

ΔG^{xs}_i is calculated in terms of integral excess Gibbs free energy of mixing (ΔG^{xs}_M) of the quinary system as [9]

$$\Delta G^{xs}_i = \Delta G^{xs}_M + \sum_{j=1}^{m} (\delta_{ij} - x_j) \frac{\partial \Delta G^{xs}_M}{\partial x_j} \quad (11)$$

where δ_{ij} is the Kronecker delta function.

2.2 Surface properties

The surface tension (σ) of a quinary liquid alloy is calculated using the analytical expression of Butler's model [11, 12, 14, 23, 26, 27]

$$\sigma = \sigma_i + \frac{RT}{A_i} \ln \frac{x^s_i}{x^b_i} + \frac{\Delta G^{xs}_{i,s} - \Delta G^{xs}_{i,b}}{A_i} \quad (12)$$

Here, $\sigma_i (i = 1, 2, 3, 4, 5)$ is the surface tension of the individual component at temperature of interest T, R is the molar gas constant, and x^s_i and x^b_i are the concentrations of the component i in the surface phase and the bulk phase respectively. $\Delta G^{xs}_{i,s}$ and $\Delta G^{xs}_{i,b}$ are respectively the partial excess free energy for the surface phase and the bulk phase of the individual component, and are related as $\Delta G^{xs}_{i,s} = \beta \Delta G^{xs}_{i,b}$ [11, 20, 26, 28] . The term β is semi-empirical parameter and its value depends upon the state and type of the atoms of the liquid mixture.

A_i is the surface area of the monolayer of one mole of pure element i and it can be calculated using the relation [23, 26]

$$A_i = f N_A^{1/3} (M_i/\rho_i)^{2/3} \quad (13)$$

where f is called geometric factor and its value depends upon the type of crystal of the atoms in the mixture and the terms N_A, M_i and ρ_i are the Avogadro's number, molar mass of element i and density of the element i respectively. The value of f is calculated from the relation [17, 23, 26]

$$f = (3 f_b/4)^{2/3} (\pi^{1/3}/f_s) \quad (14)$$

with f_b and f_s are the volume and surface packing fractions respectively.

3 Results and Discussion

3.1 Thermodynamic properties

Table 1: Interaction energy parameters of the binary sub-system of Al-Cu-Fe-Si-Ti liquid alloy

System	A^ν_{ij} [Jmol^{-1}]		Reference
Al-Cu	A^0_{ij}	-67094+8.56*T	[29]
	A^1_{ij}	32148-7.12T T	
	A^2_{ij}	5915-5.89 T	
Al-Fe	A^0_{ij}	-91976.5+22.13*T	[30]
	A^1_{ij}	-5672.58+4.8728*T	
	A^2_{ij}	121.9	
Al-Si	A^0_{ij}	-11340.1-1.23*T	
	A^1_{ij}	-3530.93+1.35993*T	
	A^2_{ij}	2265.39	
Al-Ti	A^0_{ij}	-108250+38*T	
	A^1_{ij}	-6000+5.00*T	
	A^2_{ij}	15000	
Cu-Fe	A^0_{ij}	36088-2.33*T	
	A^1_{ij}	324.53-0.0327*T	
	A^2_{ij}	324.53-0.033*T	
Cu-Si	A^0_{ij}	-39688.86+14.27*T	
	A^1_{ij}	-49937.13+29.79*T	
	A^2_{ij}	-31810.6+18.008*T	
Cu-Ti	A^0_{ij}	-19330+7.651*T	[24]
	A^1_{ij}	0	
	A^2_{ij}	9382-5.45*T	
Fe-Si	A^0_{ij}	-62273.8+5.70*T	[30]
	A^1_{ij}	-5491.468	
	A^2_{ij}	-18821.54+22.07*T	
Fe-Ti	A^0_{ij}	-164434.6 +41.98*T	
	A^1_{ij}	-21.52*T	
	A^2_{ij}	0	
Si-Ti	A^0_{ij}	-255852.17+21.87*T	
	A^1_{ij}	25025.35-2.00*T	
	A^2_{ij}	83940.65-6.71*T	

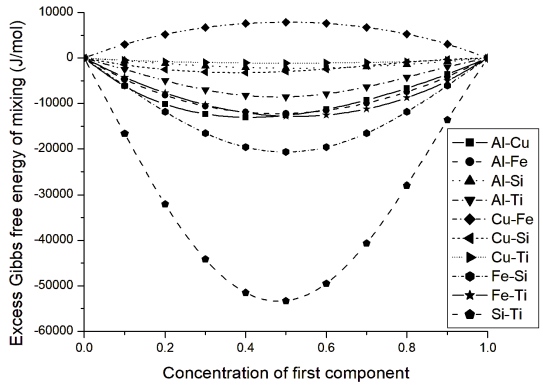

Figure 1: Excess Gibbs free energy of mixing (ΔG_{ij}^{xs}) of binary sub-systems of Al-Cu-Fe-Si-Ti liquid alloy at 1950 K

Experimental as well as theoretical studies of the binary subsystems of Al-Cu-Fe-Si-Ti are available in literature. Hultgren et al. [31] have compiled the experimental data of thermodynamic parameters of many binary subsystems, which is one of the popularly cited sources in the study of alloy. The previous studies showed that the binary sub-systems Al-Cu [32–34] , Al-Fe [23, 35–38] , Al-Si [32, 39] and Al-Ti [36, 40, 41] are ordering alloys whereas Cu-Fe sub-system is reported to have segregating nature [2, 42–44]. Additionally, Cu-Si [45], Cu-Ti [46, 47], Fe-Si [48, 49] and Si-Ti [50–52] have been investigated to have ordering nature.

The theoretical approaches applied in this study treat the thermodynamic and surface properties of a multicomponent liquid alloy as the sum of the corresponding properties of all binary subsystems, with specific weightages assigned to each. The excess parameters of a binary liquid alloy are expressed in terms of Redlich-Kister (R-K) polynomials. The optimized coefficients of the R-K polynomials for the binary subsystems of the Al-Cu-Fe-Si-Ti liquid alloy were obtained from the literature and are presented in Table 1. The excess Gibbs free energy of mixings of the binary sub-systems (ΔG_{ij}^{xs}) of the quinary liquid alloy were calculated at 1950 K using aforementioned and are plotted in Figure 1. Among the 10 binary sub-systems, Cu-Fe was found to have positive (ΔG_{ij}^{xs}) with peak value of 7.880 kJmol^{-1} at $Cu_{50}Fe_{50}$. The rest of all were found to have negative (ΔG_{ij}^{xs}) with the peak values of -13.00 kJmol^{-1} at $Al_{40}Cu_{60}$, -12.20 kJmol^{-1} at $Al_{50}Fe_{50}$, -2.230 kJmol^{-1} at $Al_{50}Si_{50}$, -8.540 kJmol^{-1} at $Al_{50}Ti_{50}$, -3.200 kJmol^{-1} at $Cu_{40}Si_{60}$, -1.100 kJmol^{-1} at $Cu_{50}Ti_{50}$, -20.60 kJmol^{-1} at $Fe_{50}Si_{50}$, -12.80 kJmol^{-1} at $Fe_{50}Ti_{50}$ and -53.30 kJmol^{-1} at $Si_{50}Ti_{50}$, Figure 1. These results indicate that the Cu-Fe subsystem is segregating in nature, whereas the others exhibit ordering behavior, with Si-Ti being the most ordering, followed by Cu-Ti, Fe-Si, Al-Cu, Al-Si, Al-Ti, Al-Fe, and Cu-Si.

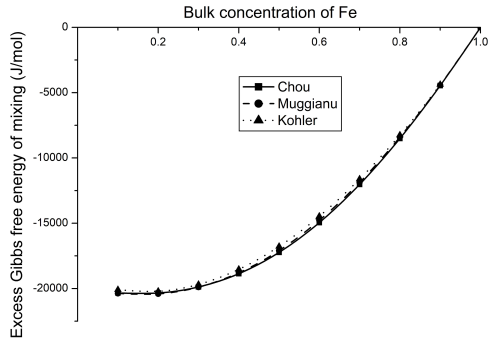

(a)

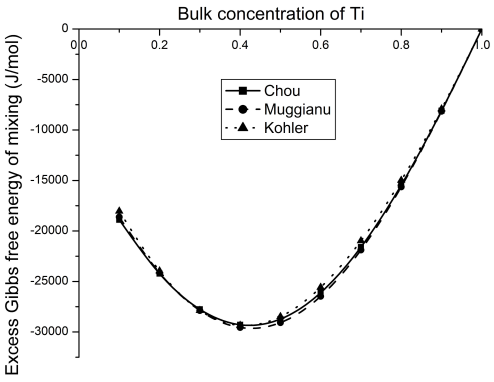

(b)

Figure 2: ΔG_M^{xs} of Al-Cu-Fe-Si-Ti liquid alloy at 1950 K from (a) Fe corner at cross-section $x_{Al} : x_{Cu} : x_{Si} : x_{Ti} = 4{:}1{:}2{:}3$ (b) Ti corner at cross-section $x_{Al} : x_{Cu} : x_{Si} : x_{Ti} = 1{:}2{:}3{:}4$.

As Cu-Fe is the only segregating subsystem and Si-Ti is the strongest ordering subsystem among all binaries, this work focuses on exploring the excess Gibbs free energy of mixing (ΔG_M^{xs}) and the activities of the components in the Al-Cu-Fe-Si-Ti liquid alloy from the Fe and Ti corners. In this regard, ΔG_M^{xs} of system was calculated at 1950 K at cross-section $x_{Al} : x_{Cu} : x_{Si} : x_{Ti} = 4{:}1{:}2{:}3$ from Fe corner and at $x_{Al} : x_{Cu} : x_{Fe} : x_{Si} = 1{:}2{:}3{:}4$ from Ti corner in the framework of Chou, Muggianu and Kohler models for comparison process. For the purpose, Equations (2-9) along with the required parameters from Table 1 have been utilized. The calculated values of ΔG_M^{xs} from the preferred models are consistent with each other (Figure 2(a,b)) thereby validating the present computational ap-

proaches.

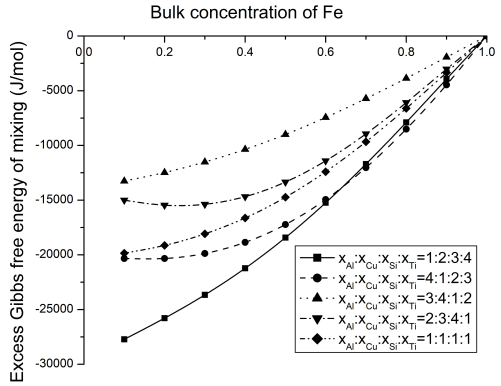

(a)

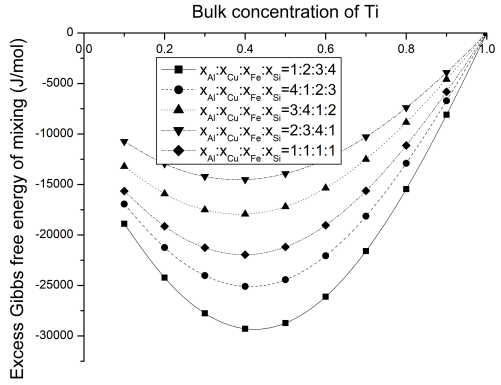

(b)

Figure 3: Compositional variations of ΔG_M^{xs} for Al-Cu-Fe-Si-Ti liquid alloy at 1950 K from (a) Fe corner (b) Ti corner at 1:2:3:4,4:1:2:3,3:4:1:2,2:3:4:1 and 1:1:1:1 fixed compositions of other atoms.

Additionally, the values of ΔG_M^{xs} were calculated from the Fe and Ti corners at fixed compositions of the remaining atoms in the ratios 1:2:3:4, 4:1:2:3, 3:4:1:2, 2:3:4:1 and 1:1:1:1 using the Chou model (Figure 3 (a,b)).The optimum values of ΔG_M^{xs} from the Fe corner were found to be -27.720, -20.340, -13.260, -15.460, and -19.580 kJmol^{-1} for the above-mentioned cross-sections $x_{Al} : x_{Cu} : x_{Si} : x_{Ti}$ =1:2:3:4,4:1:2:3,3:4:1:2,2:3:4:1 and 1:1:1:1 respectively, Figure 3(a). These results suggest that, at a particular Fe concentration, the strength of interaction between the components increases with an increase in the concentrations of Si and Ti, whereas it decreases with an increase in Cu concentration. This is because higher Si and Ti concentrations promote the formation of the most energetic and ordering complexes of Si–Ti, Fe–Si, and Fe–Ti. Conversely, increasing the Cu concentration reduces the number of ordering pairs, which lowers the magnitude of the negative ΔG_M^{xs} value. The present investigation also reveals that the strength of quinary interaction in the alloy is dominated by binary pairs interactions of Si–Ti in the cross-sections $x_{Al} : x_{Cu} : x_{Si} : x_{Ti}$=1:2:3:4, 4:1:2:3 and 1:1:1:1, Fe-Si and Fe-Ti interactions in 3:4:1:2 and 2:3:4:1.

The maximum negative values of ΔG_M^{xs} calculated from the Ti corner are -29.280, -25.010, -17.900, -14.500, and -21.950 kJmol^{-1} for the cross-sections $x_{Al} : x_{Cu} : x_{Fe} : x_{Si}$ = 1:2:3:4, 4:1:2:3, 3:4:1:2, 2:3:4:1 and 1:1:1:1 respectively, Figure 3(b). These results indicate that increment in the concentrations of Fe and Si have greater influence on increasing ΔG_M^{xs} of the system from the Ti corner. The maximum ΔG_M^{xs} values in the quinary compositions are lower than the maximum ΔG_{ij}^{xs} value of the Si-Ti binary system at the composition $Si_{50}Ti_{50}$. This suggests that the robustness of the quinary interaction is surpassed by that of the Si–Ti binary interaction. Further, the strength of the quinary interaction is dominated by Si–Ti interactions in the cross-sections 1:2:3:4, 4:1:2:3, and 1:1:1:1; by Cu–Ti, Fe—Si, and Si—Ti interactions in 3:4:1:2; and by Cu—Ti and Fe—Ti interactions in 2:3:4:1.

3.2 Activity

The activities of the components of the Al–Cu–Fe–Si–Ti liquid alloy were calculated at 1950 K and higher temperatures in the aforementioned cross-sections using Equations (10) and (11) within the framework of the Chou model. The activities of the components calculated from the Fe corner at the cross-section $x_{Al} : x_{Cu} : x_{Si} : x_{Ti}$ = 3:4:1:2 are illustrated in Figure 4(a).

It can be observed that the activity of Fe (a_{Fe}) exhibits a small negative deviation from ideal behavior, indicating its tendency to form complexes with other components. At $x_{Fe} = 0.1$, the activities are $a_{Al} = 0.10$, $a_{Cu} = 0.31$, $a_{Si} = 0.008$ and $a_{Ti} = 0.043$. As the Fe concentration increases (i.e., the concentrations of the other components decrease), the activities of Al, Si, and Ti decrease steadily, whereas the activity of Cu initially increases despite its decreasing concentration, Figure 4(a). After reaching a maximum of 0.46, a_{Cu} decreases with further increases in Fe concentration. This behavior can be explained by the segregating nature of the Cu-Fe system and the ordering tendency of the other binary subsystems. Increasing the Fe concentration favors the formation of complexes between Fe and the other elements, except Cu. Consequently, Cu shows a stronger tendency to leave the solution, which initially raises its ac-

tivity. However, at higher Fe concentrations, the very low concentrations of all other components are available in the liquid mixture, including Cu which leads to a reduction in the activities of Al, Cu, Si and Ti. Moreover, a_{Fe} increases gradually with increase in its concentration as expected.

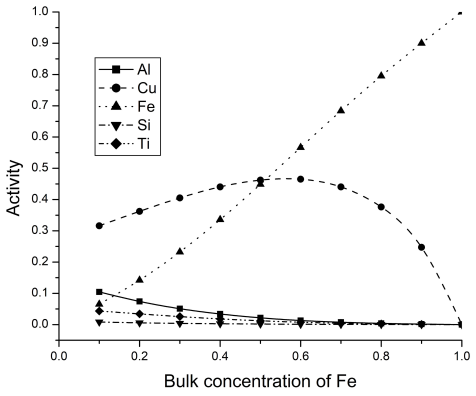

(a)

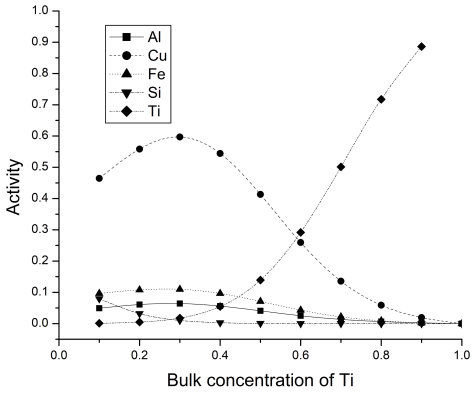

(b)

Figure 4: Activity of components of Al-Cu-Fe-Si-Ti liquid alloy at 1950 K (a) Fe corner at cross-section $x_{Al} : x_{Cu} : x_{Si} : x_{Ti} = 3{:}4{:}1{:}2$ (b) Ti corner at cross-section $x_{Al} : x_{Cu} : x_{Fe} : x_{Si} = 1{:}2{:}3{:}4$.

The activity of Ti (a_{Ti}), calculated from the Ti corner, shows a negative deviation from ideal behavior (Figure 4b), indicating its strong tendency to form complexes throughout the entire concentration range. At $x_{Ti} = 0.1$, the activities of the other components are found to be $a_{Al} = 0.05$, $a_{Cu} = 0.46$, $a_{Fe} = 0.09$ and $a_{Si} = 0.08$. With increasing Ti concentration or decreasing concentrations of Al, Cu, and Fe, the activities of Al, Cu, and Fe increased, reaching maximum values of $a_{Al} = 0.064$, $a_{Cu} = 0.599$ and $a_{Fe} = 0.110$, before decreasing again with further reductions in their respective concentrations. This trend arises from the strong complex-forming tendency of Si and Ti, as evidenced by their large negative ΔG_M^{xs}, which dominates over the weaker ordering tendencies of the other binary subsystems. At equiatomic composition, the activities follow the order $a_{Cu}>a_{Al}>a_{Fe}>a_{Ti}>a_{Si}$.

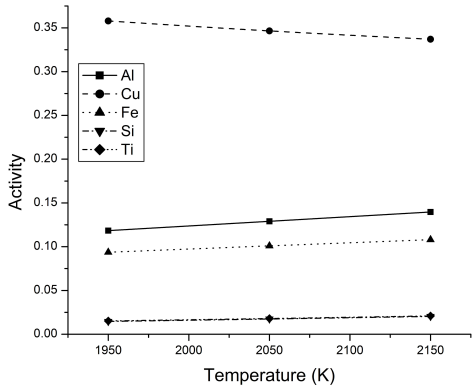

Figure 5: Variation of activity of components with temperature at composition $Al_{20}Cu_{20}Fe_{20}Si_{20}Ti_{20}$.

The variation of the component activities with temperature at equiatomic composition ($Al_{20}Cu_{20}Fe_{20}Si_{20}Ti_{20}$) was also studied in the present work. The activities of Al, Fe, Si, and Ti increase with rising temperature whereas that of Cu decreases (Figure 5). Al, Fe, Si, and Ti exhibit negative deviations from ideality, indicating their complex-forming nature in this alloy. However, this tendency diminishes at elevated temperatures, leading to an increase in their activities. In contrast, Cu shows a positive deviation from Raoult's law, reflecting its segregating behavior. Consequently, the activity of Cu decreases as temperature rises.

3.3 Surface properties

The surface tension (σ) of the liquid alloy was calculated at 1950 K and higher temperatures using the Butler equation. For this purpose, the surface tensions, densities, their temperature variations, and melting temperatures of the individual alloy components, listed in Table 2, were taken from the literature [53]. By employing these parameters along with the determined values of partial excess Gibbs free energy of mixing (ΔG_i^{xs}) of the individual components in Equations (11) and (12), the surface tension of the quinary system was evaluated from both Fe and Ti corners by varying the concentration of the corner element from 0.1 to 0.9. These values were calculated at aforementioned cross-sections as a function of concentration and are displayed in Figure 6(a,b).

Table 2: Input physical parameters for surface tension at melting temperature (T_0) [53]

Parameter	Element				
	Al	Cu	Fe	Si	Ti
T_m [K]	933	1360	1809	1683	1958
ρ_0 [kg m^{-3}]	2385	8000	7030	2524	4110
$\frac{\partial \rho}{\partial T}$ [kg m^{-3} K^{-1}]	-0.28	-0.801	-0.833	-0.3487	-0.226
σ_0 [N m^{-1}]	0.914	1.285	1.872	0.865	1.65
$\frac{\partial \sigma}{\partial T}$ [N m^{-1} K^{-1}]	-0.00035	-0.00013	-0.00049	-0.00013	-0.00026

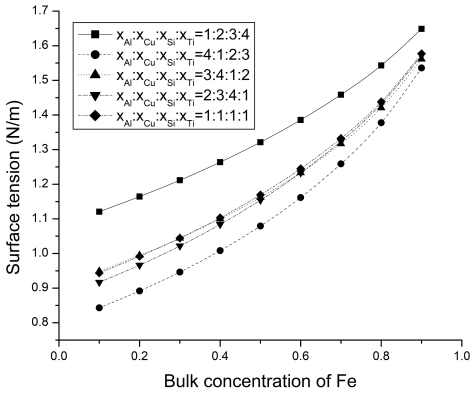

(a)

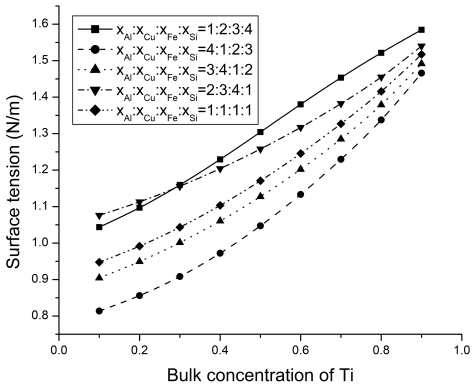

(b)

Figure 6: Surface tension of the Al-Cu-Fe-Si-Ti liquid alloy at 1950 K calculated from (a) Fe corner and (b) Ti corner.

In the Fe corner, calculations were performed for the cross-sections $x_{Al} : x_{Cu} : x_{Si} : x_{Ti}$ = 1:2:3:4, 4:1:2:3,3:4:1:2, 2:3:4:1 and 1:1:1:1, as illustrated in Figure 6(a). At x_{Fe} = 0.1, the computed σ values are 1.12, 0.84, 0.95, 0.92, and 0.94 Nm^{-1} for the respective cross-sections. With increasing bulk concentration of Fe, the surface tension of the liquid alloy gradually increases in each cross-section. Among the alloy components, Ti exhibits the highest surface tension (σ_{Ti} = 1.6487 Nm^{-1}) and Al the lowest (σ_{Al} = 0.558 Nm^{-1}) at 1950 K, Table 2. Therefore, at a given Fe concentration, the alloy's surface tension is maximized in the cross-section with the largest proportion of Ti and minimized in the cross-section with the largest proportion of Al. This demonstrates that the surface tension of the quinary liquid alloy increases with increasing Ti concentration and decreases with increasing Al concentration.

The surface tension of the liquid alloy was also calculated from the Ti corner for the cross-sections $x_{Al} : x_{Cu} : x_{Fe} : x_{Si}$ = 1:2:3:4, 4:1:2:3, 3:4:1:2, 2:3:4:1 and 1:1:1:1, shown in Figure 6(b). At x_{Ti} = 0.1, the computed values of σ are 1.043, 0.81, 0.90, 1.07, and 0.94 Nm^{-1} for the respective cross-sections. The maximum surface tension, observed at the cross-section $x_{Al} : x_{Cu} : x_{Fe} : x_{Si}$ = 2:3:4:1, is attributed to the higher proportions of Cu and Fe, both of which have relatively large surface tensions, Table 2. Conversely, the minimum surface tension is observed at the cross-section $x_{Al} : x_{Cu} : x_{Fe} : x_{Si}$ = 4:1:2:3, resulting from the lower proportions of Cu and Fe and the higher proportions of Al and Si, which have comparatively lower surface tensions. These findings demonstrate that the surface tension of the liquid alloy increases in compositions where elements with inherently higher surface tensions are present in greater proportions.

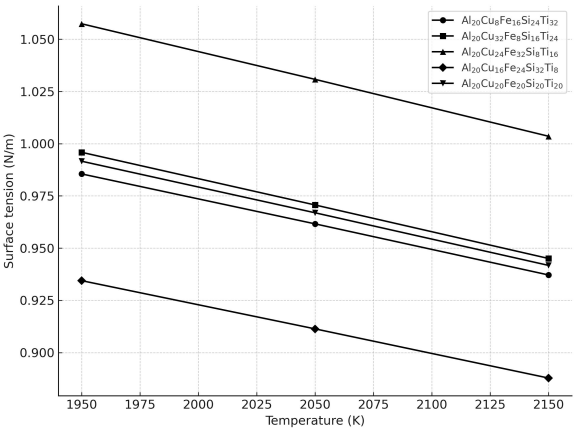

Figure 7: Variation of surface tension of Al–Cu–Fe–Si–Ti liquid alloy with temperature.

Variation of surface tension of the quinary alloy with temperature was studied at different compositions, out of which variation at five different assembly of atoms of the liquid alloy is demonstrated in Figure 7. Surface tension of the liquid alloy is observed to decrease at elevated temperature, implying the decrease in the atomic interactions among the constitute atoms of the liquid mixture. This result further justifies the the mixing tendency predicted by the previously determined thermodynamic functions of the system at elevated temperatures.

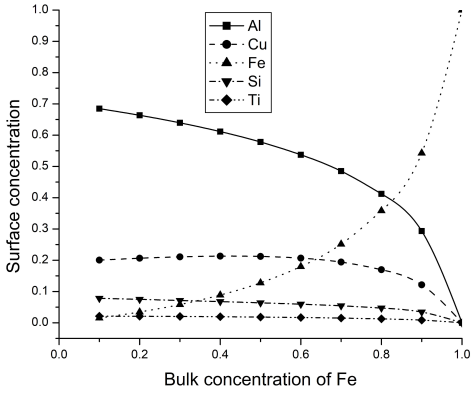

(a)

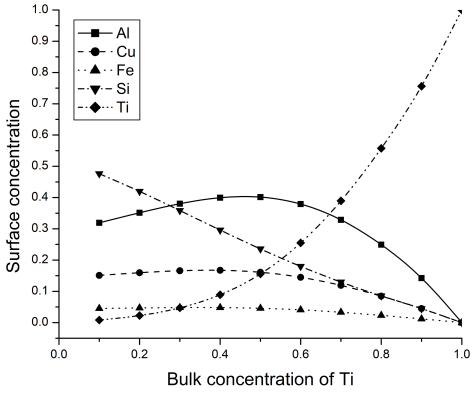

(b)

Figure 8: Surface concentrations of components of Al-Cu-Fe-Si-Ti of liquid alloy calculated from (a) Fe corner at cross-section $x_{Al} : x_{Cu} : x_{Si} : x_{Ti}$ = 3:4:1:2 (b) Ti corner at cross-section $x_{Al} : x_{Cu} : x_{Fe} : x_{Si}$ = 1:2:3:4.

The surface concentrations of the components $(x_i^s, i = Al, Cu, Fe, Si, Ti)$ of the quinary system were computed as a function of Fe and Ti concentrations in different cross-sections. As shown in Figure 8(a), at the cross-section $x_{Al} : x_{Cu} : x_{Si} : x_{Ti}$ = 3:4:1:2, the surface concentrations of atoms at 1950 K are found to be x_{Al}^s = 0.66359, x_{Cu}^s = 0.20645, x_{Fe}^s = 0.0.034397, x_{Si}^s = 0.07484 and x_{Ti}^s = 0.020699, while the corresponding bulk concentrations are x_{Al} = 0.24, x_{Cu} = 0.32, x_{Fe} = 0.20, x_{Si} = 0.08 and x_{Ti} = 0.16. These results indicate a strong tendency of Al atoms to segregate at the surface, while the other atoms preferentially remain in the bulk phase. The surface concentration of Fe increases gradually at first and then rises sharply with increasing bulk Fe concentration. In contrast, the surface concentration of Al decreases markedly, whereas Si and Ti concentrations decrease gradually. Interestingly, the surface concentration of Cu initially increases despite a decrease in its bulk concentration, but after reaching a maximum value, it decreases again. This unusual behavior of Cu can be attributed to the strong ordering tendency of the other elements with Fe, which reduces the likelihood of Cu forming bonds with them. As a result, Cu atoms preferentially migrate toward the surface phase. A similar variation in the surface concentration of Al atoms has been reported in the Ti-Al-Si ternary liquid alloy by Yadav et al. [28].

In the Ti corner at the cross-section $x_{Al} : x_{Cu} : x_{Fe} : x_{Si}$ = 1:2:3:4, the surface concentrations are found to be x_{Al}^s = 0.351316, x_{Cu}^s = 0.159499, x_{Fe}^s = 0.04691, x_{Si}^s = 0.419739 and x_{Ti}^s = 0.022489, corresponding to bulk concentrations of x_{Al} = 0.08, x_{Cu} = 0.16, x_{Fe} = 0.24, x_{Si} = 0.32 and x_{Ti} = 0.20 (Figure 8(b)). In this region, Al and Si exhibit a strong tendency to segregate into the surface phase, while Cu, Fe, and Ti preferentially remain in the bulk phase. Moreover, the surface concentration of Ti increases gradually at first and then rises sharply with increasing bulk Ti concentration. Conversely, x_{Si}^s decreases as bulk concentration of Ti increases. The concentrations of Al, Cu, and Fe at the surface initially rise with decreasing bulk concentration, reaching a peak before declining again. This unusual behavior is attributed to the dominant presence of Si and the strong ordering tendency of the Si-Ti system, which influences the distribution of Al, Cu and Fe at the surface. At equiatomic composition, the overall extent of surface segregation tendency of the alloying elements follows the order Al>Si>Cu>Fe>Ti>.

We have also calculated the temperature dependence of the surface concentrations at a fixed composition, $Al_{20}Cu_{20}Fe_{20}Si_{20}Ti_{20}$, Figure 9. The surface surface concentrations of the components at this composition are found to be x_{Al}^s = 0.620774, x_{Cu}^s = 0.139894, $x^s Fe$, = 0.031593, x_{Si}^s = 0.186671 and x_{Ti}^s = 0.021066 at 1950 K. This implies the highest surface segregating nature of Al and lowest surface segregating nature of Ti among the components in this composition too. Further, the surface concentration of Fe and Ti appears to be en-

hanced with rise in temperature, whereas, surface concentration of Al, Cu and Si appears to decrease at higher temperature.

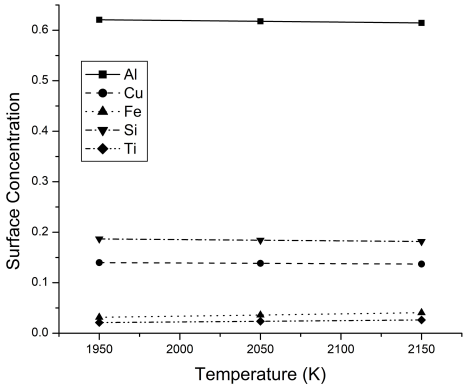

Figure 9: Variation of surface concentrations of the components of Al–Cu–Fe–Si–Ti liquid alloy with temperature.

4 Conclusion

The thermodynamic analysis of the Al-Cu-Fe-Si-Ti liquid alloy reveals that its multicomponent behavior is primarily governed by the interactions within its binary subsystems. Among the ten binaries, Cu-Fe exhibits a segregating tendency with positive excess Gibbs free energy of mixing, while the remaining systems show ordering behavior, with Si-Ti being the strongest ordering pair. The calculated quinary ΔG_M^{xs} values from both Fe and Ti corners confirm the consistency of Chou, Muggianu, and Kohler models, thereby validating the present computational approach. The quinary alloy exhibits stronger negative ΔG_M^{xs} values when Si and Ti concentrations are high, emphasizing the dominance of Si-Ti, Fe-Si, and Fe-Ti interactions. Conversely, higher Cu concentration reduces ordering, leading to weaker interactions. Comparison with binary interactions shows that the robustness of quinary ordering does not surpass the strong Si-Ti binary interaction at 1950 K. Overall, the alloy's thermodynamic stability is strongly influenced by the cooperative effects of ordering pairs, particularly Si-Ti, Fe-Si, and Fe-Ti, while Cu tends to weaken the interaction strength due to its segregating nature with Fe. This tendency of the quinary system is further justified by the results of activity, the other thermodynamic function. The surface tension of the quinary system increases at each cross-section with the increase in concentrations of Fe and Ti. The surface tension rises in alloy compositions enriched with elements that naturally possess higher surface tensions. At the cross-section $x_{Al} : x_{Cu} : x_{Si} : x_{Ti} = 3{:}4{:}1{:}2$ and from Fe corner, Al atoms segregate at the surface, while the other atoms preferentially remain in the bulk phase. From Ti corner at $x_{Al} : x_{Cu} : x_{Fe} : x_{Si}$=1:2:3:4, Al and Si exhibit a strong tendency to segregate into the surface phase, while Cu, Fe, and Ti preferentially remain in the bulk phase. At equiatomic composition, the overall extent of surface segregation tendency of the alloying elements follows the order Al>Si>Cu>Fe>Ti>. Temperature elevation systematically decreases both surface segregation and deviations in activities, confirming that the system approaches an ideal random distribution at higher temperatures.

References

[1] C. Corti. 22nd Santa Fe Symposium On Jewellery Manufacturing Technology, 18–21 May 2008 Albuquerque, New Mexico, USA. *Gold Bulletin*, 41(3):269–271, 2008.

[2] H. Nishimura and C. Hisatsune. The constitution of the alloys of copper, aluminium, and iron. *Memoirs of the College of Engineering, Kyoto Imperial University*, 10(5):163–172, 1939.

[3] R. Babilas, A Bajorek, M. Spilka, A. Radoń, and W. Łoński. Structure and corrosion resistance of Al–Cu–Fe alloys. *Progress in Natural Science: Materials International*, 30(3):393–401, 2020.

[4] A.P. Tsai, A. Inoue, and T. Masumoto. Effects of preparation conditions and additional elements on phason strains in stable icosahedral quasicrystals in Al-Cu-Fe systems. *Journal of Materials Science Letters*, 8(4):470–472, 1989.

[5] M. Mitka, A. Góral, and L. Lityńska-Dobrzyńska. Synthesis and stability of quasicrystalline phase in Al-Cu-Fe-Si mechanically alloyed powders. *Journal of Materials Science*, 56(18):11071–11082, 2021.

[6] S. Khalesi, R. Omidi, R. Taghiabadi, and M. Emami. Effect of Si addition on the weibull distribution of tensile properties of fe-bearing Al-Cu alloys. *Silicon*, 16(11):4609–4620, 2024.

[7] T. Moskalewicz, M. Kot, and B. Wendler. Microstructure development and properties of the AlCuFe quasicrystalline coating on near-α titanium alloy. *Applied Surface Science*, 258(2):848–859, 2011.

[8] Y. Ouyang, X. Zhong, Y. Du, Y. Feng, and Y. He. Enthalpies of formation for the Al–Cu–Ni–Zr quaternary alloys calculated via a combined approach of geometric model and

miedema theory. *Journal of Alloys and Compounds*, 420(1-2):175–181, 2006.

[9] H. Arslan and A. Dogan. An analytical investigation for thermodynamic properties of the Fe-Cr-Ni-Mg-O system. *Russian Journal of Physical Chemistry A*, 89(2):180–189, 2015.

[10] M. Hillert. Partial gibbs energies from redlich-kister polynomials. *Thermochimica acta*, 129(1):71–75, 1988.

[11] A. Dhungana, S.K. Yadav, and D. Adhikari. Thermodynamic and surface properties of Al–Li–Mg liquid alloy. *Physica B: Condensed Matter*, 598:412461, 2020.

[12] H. Arslan and A. Dogan. Determination of surface tension of liquid ternary Ni–Cu–Fe and sub-binary alloys. *Philosophical Magazine*, 99(10):1206–1224, 2019.

[13] A. Dogan, H. Arslan, and T. Dogan. Estimation of excess energies and activity coefficients for the penternary Ni-Cr-Co-Al-Mo system and its subsystems. *The Physics of Metals and Metallography*, 116(6):544–551, 2015.

[14] U. Mehta, S.K. Yadav, I. Koirala, R.P. Koirala, and D. Adhikari. Thermodynamic and surface properties of liquid Ti–Al–Fe alloy at different temperatures. *Physics and Chemistry of Liquids*, 59(4):585–596, 2021.

[15] K.C. Chou. A new solution model for predicting ternary thermodynamic properties. *Calphad*, 11(3):293–300, 1987.

[16] K.C. Chou. A general solution model for predicting ternary thermodynamic properties. *Calphad*, 19(3):315–325, 1995.

[17] U. Mehta, S.K. Yadav, I. Koirala, R.P. Koirala, G.K. Shrestha, and D. Adhikari. Study of surface tension and viscosity of Cu–Fe–Si ternary alloy using a thermodynamic approach. *Heliyon*, 6(8), 2020.

[18] C. Costa, S. Delsante, G. Borzone, D. Zivkovic, and R. Novakovic. Thermodynamic and surface properties of liquid Co–Cr–Ni alloys. *The Journal of Chemical Thermodynamics*, 69:73–84, 2014.

[19] J. Wang, P. Hudon, D. Kevorkov, C. Patrice, I.H. Jung, and M. Medraj. Thermodynamic and experimental study of the Mg-Sn-Ag-In quaternary system. *Journal of Phase Equilibria and Diffusion*, 35(3):284–313, 2014.

[20] D.K. Sah, U. Mehta, D. Adhikari, and S.K. Yadav. Model based study of temperature dependent thermodynamic and surface properties of Al-Ti-Ni-Cr system in liquid state. *Physica B: Condensed Matter*, 695:416471, 2024.

[21] D.K. Sah, U. Mehta, R.K. Gohivar, D. Adhikari, and S.K. Yadav. Theoretical assessment of thermodynamic and surface properties of Ag–Al–Au–Cu liquid alloy at different temperatures. *Applied Physics A*, 131(2):144, 2025.

[22] A. Dogan and H. Arslan. Assessment of thermodynamic properties of lead-free soldering Co–Sb–Sn, Ag–In–Pd–Sn, and Ni–Cr–Co–Al–Mo–Ti–Cu alloys. *Physics of Metals and Metallography*, 119(10):976–992, 2018.

[23] S.K. Yadav, L.N. Jha, and D. Adhikari. Modeling equations to predict the mixing behaviours of Al- Fe liquid alloy at different temperatures. *Bibechana*, 15:60–69, 2018.

[24] R. Arroyave, T.W. Eagar, and L. Kaufman. Thermodynamic assessment of the Cu–Ti–Zr system. *Journal of Alloys and Compounds*, 351(1-2):158–170, 2003.

[25] M. Hillert. Empirical methods of predicting and representing thermodynamic properties of ternary solution phases. *Calphad*, 4(1):1–12, 1980.

[26] G. Kaptay. Improved derivation of the butler equations for surface tension of solutions. *Langmuir*, 35(33):10987–10992, 2019.

[27] J.A.V. Butler. The thermodynamics of the surfaces of solutions. *Proceedings of the Royal Society of London. Series A, Containing Papers of a Mathematical and Physical Character*, 135(827):348–375, 1932.

[28] S.K. Yadav, U. Mehta, and D. Adhikari. Optimization of thermodynamic and surface properties of ternary Ti–Al–Si alloy and its sub-binary alloys in molten state. *Heliyon*, 7(3), 2021.

[29] V.T. Witusiewicz, U. Hecht, S.G. Fries, and S. Rex. The Ag–Al–Cu system: Part i: Reassessment of the constituent binaries on the basis of new experimental data. *Journal of Alloys and Compounds*, 385(1-2):133–143, 2004.

[30] I. Ansara, A.T. Dinsdale, and M.H. Rand. *Thermochemical database for light metal alloys*. Office for Official Publications of the European Communities, 1998.

[31] R.R. Hultgren, P.D. Desai, D.T. Hawkins, M. Gleiser, K.K. Kelley, and D.D. Wagman. Selected values of the thermodynamic properties of binary alloys (ASM, Metals Park, OH, 1973). *Search in*, 2007.

[32] DS Kanibolotsky, OA Bieloborodova, NV Kotova, and VV Lisnyak. Thermodynamic properties of liquid al-si and Al-Cu alloys. *Journal of Thermal Analysis and Calorimetry*, 70(3):975–983, 2002.

[33] R.K. Mishra, R. Lalneihpuii, and R. Venkatesh. Statistical mechanical studies of Al rich Al–Cu melts. *Physica A: Statistical Mechanics and its Applications*, 550:123901, 2020.

[34] M. Trybuła, N. Jakse, W. Gąsior, and A. Pasturel. Thermodynamics and concentration fluctuations of liquid Al-Cu and Al-Zn alloys. *Archives of Metallurgy and Materials*, 60(2A):649–655, 2015.

[35] A. Walnsch, M.J. Kriegel, O. Fabrichnaya, and A. Leineweber. Thermodynamic assessment and experimental investigation of the systems Al–Fe–Mn and Al–Fe–Mn–Ni. *Calphad*, 66:101621, 2019.

[36] A. Kostov, B. Friedrich, and D. Živković. Thermodynamic calculations in alloys Ti-Al, Ti-Fe, Al-Fe and Ti-Al-Fe. *Journal of Mining and Metallurgy, Section B: Metallurgy*, 44(1):49–61, 2008.

[37] I.B. Bhandari, N. Panthi, S. Gaire, and I. Koirala. Effect of temperature on mixing behavior and stability of liquid Al-Fe alloys. In *Journal of Physics: Conference Series*, volume 2070, page 012025. IOP Publishing, 2021.

[38] D. Adhikari, S.K. Yadav, and L.N. Jha. Thermo-physical properties of Al–Fe melt. *Journal of the Chinese Advanced Materials Society*, 2(3):149–158, 2014.

[39] M. Bonnet, J. Rogez, and R. Castanet. Emf investigation of Al-Si, Al-Fe-Si and Al-Ni-Si liquid alloys. *Thermochimica acta*, 155:39–56, 1989.

[40] R. Novakovic, D. Giuranno, E. Ricci, A. Tuissi, R. Wunderlich, H.J. Fecht, and I. Egry. Surface, dynamic and structural properties of liquid Al–Ti alloys. *Applied Surface Science*, 258(7):3269–3275, 2012.

[41] R.G. Reddy, A.M. Yahya, and L. Brewer. Thermodynamic properties of Ti–Al intermetallics. *Journal of Alloys and Compounds*, 321(2):223–227, 2001.

[42] Y. Chuang, R. Schmid, and Y.A. Chang. Thermodynamic analysis of the iron-copper system i: The stable and metastable phase equilibria. *Metallurgical Transactions A*, 15(10):1921–1930, 1984.

[43] M.A. Turchanin, P.G. Agraval, and I.V. Nikolaenko. Thermodynamics of alloys and phase equilibria in the copper-iron system. *Journal of Phase Equilibria*, 24(4):307–319, 2003.

[44] Q. Chen and Z. Jin. The Fe-Cu system: A thermodynamic evaluation. *Metallurgical and Materials Transactions A*, 26(2):417–426, 1995.

[45] X. Yan and Y.A. Chang. A thermodynamic analysis of the Cu–Si system. *Journal of Alloys and Compounds*, 308(1-2):221–229, 2000.

[46] T. Abbas and A.B. Ziya. Evidence of short-range order in the disordered Cu-Ti alloys. *Journal of Materials Science*, 28(18):5010–5013, 1993.

[47] P. Wei and L. Jie. Thermodynamics of Ti in Cu–Ti alloy investigated by the emf method. *Materials Science and Engineering: A*, 269(1-2):104–110, 1999.

[48] D. Kanibolotsky, O. Bieloborodova, N. Kotova, and V. Lisnyak. Thermodynamics of liquid Fe-Si and Fe-Ge alloys. *Journal of Thermal Analysis and Calorimetry*, 71(2):583–591, 2003.

[49] D. Adhikari, I.S. Jha, and B.P. Singh. Structural asymmetry in liquid Fe–Si alloys. *Philosophical Magazine*, 90(20):2687–2694, 2010.

[50] O.E. Awe, Y.A. Odusote, L.A. Hussain, and O. Akinlade. Temperature dependence of thermodynamic properties of Si–Ti binary liquid alloys. *Thermochimica Acta*, 519(1-2):1–5, 2011.

[51] S.H. Tabaian, M. Maeda, T. Ikeda, and Y. Ogasawara. Thermodynamic study of molten Si-Ti binary alloys. *High Temperature Materials and Processes*, 19(3-4):257–264, 2000.

[52] S.K. Yadav, U. Mehta, R.K. Gohivar, A. Dhungana, R.P. Koirala, and D. Adhikari. Reassessments of thermo-physical properties of Si-Ti melt at different temperatures. *Bibechana*, 17:146–153, 2020.

[53] J.J. Valencia and P.N. Quested. Thermophysical properties. *Modeling for Casting and Solidification Processing*, 189, 2001.